

CONTENTS – W through Z

The Location of Martian Atmospheric Argon in Three Martian Basalts: Controls Exerted by Shock Effects <i>E. L. Walton, S. P. Kelley, and J. G. Spray</i>	5182
Core Formation in Planetesimals: Constraints from Siderophile Elements in Ureilites <i>P. H. Warren</i>	5223
Lunar Meteorite Yamato-983885: A Relatively KREEPy Regolith Breccia Not Paired with Y-791197 <i>P. H. Warren and J. C. Bridges</i>	5095
Extensive Melting of Amoeboid-Olivine Inclusions <i>J. T. Wasson, A. E. Rubin, and J. M. Trigo-Rodriguez</i>	5202
Fabric Analysis of Allende Matrix Using EBSD <i>L. E. Watt, P. A. Bland, S. S. Russell, and D. J. Prior</i>	5037
Unraveling the Exposure Histories of Aubrites <i>K. C. Welten, K. Nishiizumi, D. J. Hillegonds, M. W. Caffee, and J. Masarik</i>	5220
Nitrogen-Mapping and Nitrogen-XANES Spectroscopy of Interplanetary Dust Particles <i>S. Wirick, G. J. Flynn, L. P. Keller, and C. Jacobsen</i>	5092
Further Analysis of the Pd-Ag Systematics of Sulphides from the Group IA Iron Meteorite Canyon Diablo <i>S. J. Woodland, M. Rehkämper, and A. N. Halliday</i>	5036
Evaluation of the Meteoritic Alteration Level Using the Solid-State CP/MAS ¹³ C NMR Analyses of Macromolecular Material in the Antarctic Carbonaceous Chondrites <i>H. Yabuta, H. Naraoka, K. Sakanishi, and H. Kawashima</i>	5040
Basaltic Clasts in Lunar Highland Breccia Yamato 86032 <i>A. Yamaguchi, H. Takeda, Y. Karouji, and M. Ebihara</i>	5114
A Test of Image Process Procedures of Asteroid Imaging Camera by Using Its Prototype Model of Hayabusa (MUSES-C) <i>A. Yamamoto, J. Saito, M. Ishiguro, F. Yoshida, S. Hasegawa, H. Demura, S. Kobayashi, E. Nemoto, Y. Murai, K. Nishiyama, M. Furuya, and the AMICA Science Team</i>	5116
Significant Depletion of Argon-rich Noble Gases in the Ningqiang Carbonaceous Chondrite During Experimental Aqueous Alteration <i>Y. Yamamoto, R. Okazaki, and T. Nakamura</i>	5069
Metallographic Cooling Rate Methods: Applicability to Specific Temperature Ranges During Cooling <i>J. Yang and J. I. Goldstein</i>	5023
Impact Glasses as Chronostratigraphic Benchmarks of the Late Cenozoic Pampean Record, Argentina <i>M. A. Zárate, P. H. Schultz, W. Hames, C. Heil, and J. King</i>	5199

APXS Analyses of Bounce Rock — The First Shergottite on Mars <i>J. Zipfel, R. Anderson, J. Brückner, B. C. Clark, G. Dreibus, T. Economou, R. Gellert, G. Klingelhöfer, G. W. Lugmair, D. Ming, R. Rieder, S. W. Squyres, C. d'Uston, H. Wänke, A. Yen, and the Athena Science Team</i>	5173
Fluid Inclusions in Chondrites <i>M. Zolensky, R. Bodnar, A. Tsuchiyama, K. Okudaira, T. Noguchi, K. Uesugi, and T. Nakano</i>	5103
Pathways of Hydrogen Generation During Aqueous Alteration of Chondrites <i>M. Yu. Zolotov and E. L. Shock</i>	5222
Brazilian Meteorites <i>M. E. Zucolotto and L. L. Antonello</i>	5089
The São João Nepomuceno, IVA Stony-Iron <i>M. E. Zucolotto and L. L. Antonello</i>	5090

THE LOCATION OF MARTIAN ATMOSPHERIC ARGON IN THREE MARTIAN BASALTS: CONTROLS EXERTED BY SHOCK EFFECTS. E.L. Walton¹, S.P. Kelley², and J.G. Spray¹. ¹Planetary and Space Science Centre, University of New Brunswick, Canada. ²Department of Earth Sciences, The Open University, Milton Keynes, U.K. ¹E-mail: j5rng@unb.ca.

Introduction: The application of Ar-Ar dating using the laser spot fusion technique is ideal for the analysis of meteorites because of the capability to analyse small, heterogeneous samples *in situ* [1]. The objective of this study is to measure Ar isotopes within selected martian meteorites, at a resolution sufficient to distinguish the signatures of igneous minerals from localized shock-produced melts. Both shock veins and melt pockets were likely formed during the same shock event associated with ejection. However, they have different mechanisms of formation.

Samples and Methods: Ar-Ar measurements on one basalt (Zagami) and two olivine-phyric basalts (DaG 476 and NWA 1183) are reported. The dated component of each meteorite (0.25 mm thick, 1 cm² polished tile), was photographed to provide a map of the distribution of shock veins and melt pockets, and their relationship to host rock minerals. Following irradiation, ninety-nine samples were extracted from individual igneous minerals and shock features using one to three 1 ms – 3 s laser pulses. Laser melt spots 100 - 500 μm diameter resulted.

Results: *Zagami:* Matrix analyses yield a scattered array with apparent ages ~ 250-350 Ma with low concentrations of ³⁶Ar. Shock veins show a similar range of ages and ³⁶Ar contents. Melt pockets, however, exhibit over an order of magnitude greater concentrations of ³⁶Ar, with apparent ages as high as 4.3 Ga. However, ⁴⁰Ar/³⁶Ar ratios in the range 1700-1860 and ³⁶Ar/³⁸Ar ratios, consistent with martian atmosphere [2], indicate that the ages are the result of high concentrations of trapped atmosphere in the melt pockets.

NWA 1183: Matrix minerals in NWA 1183 did not yield an isochron but ‘ages’ range from ~200 Ma to > 930 Ma. Shock veins yield older apparent ages in the range 800-1250 Ma, and melt pockets in the range 2 – 4 Ga. ³⁶Ar concentrations in melt pockets are also at least an order of magnitude greater than matrix, but, in common with the apparent ages, ³⁶Ar concentrations in shock veins are intermediate between those in the matrix and melt pockets. ⁴⁰Ar/³⁶Ar ratios in the melt pockets exhibit a significant range from 900 to over 1600.

DaG 476: Matrix analyses, again, do not yield an isochron but range from ~ 500 Ma - 2 Ga. Shock veins exhibit apparent ages in the range 1 – 2.8 Ga and melt pockets are generally slightly lower than those seen in Zagami and NWA 1183. ³⁶Ar concentrations in the matrix are higher, probably as a result of terrestrial atmospheric contamination coupled with the need to analyze larger samples because of the low K contents.

Cosmic ray exposure ages measured on Zagami (3.0 ± 0.25 Ma) and NWA 1183 (2.2 ± 0.2 Ma) are within the range of those previously determined [3, 4]. DaG 476, however, yielded a young apparent age (0.7 ± 0.25 Ma), compared to data reported by [5], probably related to excess calcium in carbonate veins.

Conclusion: The inclusion of martian atmosphere into martian basalts seems to be controlled by shock features, in particular the larger melt pockets, although their amorphous nature makes them particularly susceptible to terrestrial alteration.

References: [1] Kelley 1995. *Micro. Tech. Earth Sci.* pp. 327-358. [2] Bogard and Garrison 1999. *MAPS* 34:451-473. [3] Eugster et al. 2002. *MAPS* 37:1345-1360. [4] Marty et al. 2003. *NIPS* [5] Nyquist et al. 2001. *Space Sci. Rev.* 96:105-164.

CORE FORMATION IN PLANETESIMALS: CONSTRAINTS FROM SIDEROPHILE ELEMENTS IN UREILITES

Paul H. Warren, Institute of Geophysics and Planetary Physics, University of California, Los Angeles, CA 90095-1567 USA

An important issue in models of core formation is the mechanism for metal separation, and in particular the thermal-anatctic “threshold” at which the mechanism begins to operate. It has recently been assumed [1] or argued [2] that the threshold is very low, and planetesimals separate their cores at [1] or only slightly above [2] the temperature of the Fe-FeS eutectic (~990°C). Siderophile elements are sensitive tracers of this metal-silicate segregation processes, and ureilites are residues of low- f_{O_2} asteroidal mantle partial melting sufficient to virtually eliminate the basaltic (plag) component, at temperatures of ~1210-1300°C [3]. I have determined several highly siderophile elements (Ir, Os, Au, Ni; in some cases also Re and Ru) in 19 ureilites, including some with unusually high- mg olivine and pyroxene compositions. Including literature data [e.g., 4-5], we now have constraints for Ir in some 41 ureilites (and for Ni in 44, and for Au in 36). The concentrations of Ir, Ni and Au in ureilites are very high in relation to INAA detection limits, so the analytical precision of the analyses should be excellent.

The data show that all ureilites have undergone siderophile element depletion (vs. chondrites), but the depletion factors are not at all uniform, and are on average relatively mild (e.g., the ureilites' average Ir is merely depleted to ~1/3-2/3 times the different chondrite compositions; Ni is depleted to ~1/10). Nor are they particularly systematic, in relation to known or proposed genetic subgroups among ureilites. One popular model of ureilite petrogenesis [e.g., 3, 6] assumes that most of their diversity in terms of silicate mg arose through an equilibrium smelting process, i.e., essentially by the reaction $C + MgFeSiO_4 = MgSiO_3 + Fe(metal) + CO$. If the full range of silicate mg is to be engendered by this model, the implied yield of Fe-metal is ~11 wt%. This model is testable through siderophile elements. It implies that the most magnesian ureilites should either be metal-enriched, or depleted in Ir (if Fe-metal formed but also segregated away). But ureilites like ALH84106 (Fo₉₆) and Y-791538 (Fo_{91.5}) are neither metal-rich nor Ir-poor; their Ir concentrations are nondescript: 155 [4] and 233 ng/g, respectively. The equilibrium smelting model is also implausible because the implied yield of CO(gas) is grossly in excess of what could be sustained within an intact asteroidal mantle [7].

The mild, nonsystematic siderophile depletions may reflect minor escape of some mixture of Fe-FeS eutectic melt plus (extremely minor) entrained Fe-metal. Nearly all ureilites show enhanced Ir/Au and Ir/Ni (vs. chondrites), by average factors of ~3-4. This could plausibly be a result of an outward-percolation process dominated by S-rich metallic melt, which has a higher affinity for Au and Ni than for Ir [8]. In general, these results suggest that core segregation may be a subtle, complex physical process.

References: [1] Ghosh A. & McSween H. Y, Jr. (1999) *Icarus* 134, 187. [2] Yoshino T. et al. (2003) *Nature* 422, 154. [3] Singletary S. J. & Grove T. L. (2003) *MaPS* 38, 95. [4] Warren P. H. & Kallemeyn (1992) *Icarus* 100, 110. [5] Spitz A. H. & Boynton W. V. (1991) *GCA* 55, 3417. [6] Goodrich C. A. et al. (2002) *LPS XXXIII*, 1379. [7] Warren P. H. (1996) *Meteoritics* 31, A146. [8] Chabat N. L. & Jones J. H. (2003) *MaPS* 38, 1425.

LUNAR METEORITE YAMATO-983885: A RELATIVELY KREEPY REGOLITH BRECCIA NOT PAIRED WITH Y-791197

P. H. Warren¹ and J. C. Bridges², ¹Institute of Geophysics, University of California, Los Angeles, CA 90095-1567 USA, ²PSSRI, Open University, Milton Keynes, MK7 6AA, UK.

Lunar meteorite Yamato-983885 is a 288 g highland regolith breccia [1] with mineral compositions similar to those of another Yamato lunaite regolith breccia, Y-791197. We have studied it petrographically and analyzed a 220-mg bulk-rock chip.

Our bulk-analysis results agree with those of [1] in indicating a relatively low-Al₂O₃ (22.3 wt%) variety of lunar highland material. Ratios such as Fe/Mn and especially Ga/Al further confirm the stone's lunar origin. Concentrations of siderophile elements Ni, Ir and Au are exceptionally high (e.g., Ir = 22 ng/g) and in approximately chondritic proportions to one another. In a ~1 cm² thin section, we identified ~15 glassy regolith spherules and spherule fragments. These spherule-abundance and siderophile results imply at least moderate regolith maturity, for a lunar regolith breccia, i.e., that the material is probably well mixed, with a bulk composition fairly representative of the terrain where the rock originally formed. Noble gas data [e.g., 2] indicate that Y-791197 is also relatively mature. Thus, if Y-983885 and Y-791197 were paired, we would not expect to find a very high degree of compositional-petrologic disparity between them.

Most significant for testing the Y-983885 - Y-791197 pairing hypothesis is a whopping disparity in the levels of incompatible (KREEP-associated) trace elements. Like most lunaite highland regolith breccias, Y-791197 is very KREEP-poor, with a mass-weighted literature mean Th concentration of just 0.33 µg/g. The five literature analyses averaged [3] are relatively uniform, with a range for Th of 0.27 to 0.40 µg/g. Yet the incompatible elements are consistently ~5 times more enriched in Y-983885 than in the Y-791197 average. The greatest of these disparities are by factors of 5.8-6.1, for the two most extremely incompatible elements, U and Th. This degree of compositional disparity greatly exceeds what could reasonably be expected from heterogeneity within a single moderately mature lunar regolith breccia.

In terms of incompatible trace elements, a very close precedent for the composition of Y-983885 is the average soil [3] from the prototypical nearside highland site, Apollo 16. However, the Y-983885 regolith is significantly less anorthositic than that at Apollo 16 (Al₂O₃ consistently ~ 27.1 wt%). Y-983885 is many respects similar to the KREEPy Calalong Creek regolith breccia lunaite [4], especially in terms of major elements and mafic-associated elements such as Mn, Cr, Sc and V (our results in µg/g: 950, 1430, 19.8 and 45, respectively).

An evolved (KREEP?) component is also evident in the petrography of Y-983885. For example, one of the largest clasts found (~400 × 200 µm) consists of roughly (in vol%) 40% ilmenite, 25% mesostasis, 20% Na-rich plag (An₅₁₋₆₂), 10% K-feldspar, ~4% intergrowth of K-spar with silica, and ~2% merrillite.

We will also discuss implications of these and other recent results for lunitates, for issues such as calibration of the bulk-Moon Th map and estimation of the bulk-Moon composition.

References: [1] Kaiden H. & Kojima H. (2002) *LPS* **33**, 1958. [2] Bischoff A. et al. (1987) *Proc. (NIPR) Sym. Ant. Met.*, **11th**, 21-42. [3] Warren P. H. (2004) in *Treatise on Geochemistry, Vol. 1, Meteorites, Comets, Planets* (A. M. Davis, ed.), 559-599. [4] Hill D. H. & Boynton W. V. (2003) *MaPS* **38**, 595-626.

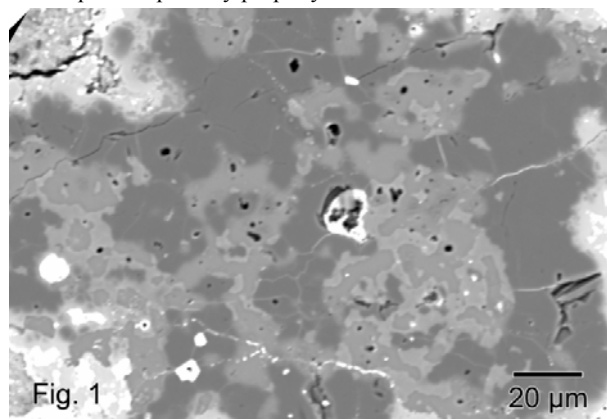
EXTENSIVE MELTING OF AMOEBOID-OLIVINE INCLUSIONS.

John T. Wasson, Alan E. Rubin and Josep M. Trigo-Rodriguez,
University of California, Los Angeles, CA 90095-1567 USA.

In CO3.0 chondrites amoeboid olivine inclusions (AOIs) typically consist of ~50-80% olivine with the remainder anorthite and diopside; some AOIs contain spinel. $\Delta^{17}\text{O}$ values in CO3.0 AOIs are $\leq -20\%$, genetically linking them to refractory inclusions.

The classical view has been that AOIs consist of sintered aggregates of grains; sintering involves melt fractions $<10\%$ and porosity at grain boundaries. AOI textures, however, show continuous phase interfaces, more consistent with extensive melting. Fig. 1 shows an AOI from CO3.0 Acfer 094. The darkest phase is olivine, lighter gray is diopside and darker gray is anorthite. Small white grains are metal. In accord with the Fo-An-Di phase diagram, olivine crystallized first, followed by anorthite or diopside depending on the bulk Ca/Al ratio; olivine forms chains of 3-10 μm crystals. There is appreciable (5-10%) porosity; pores are rounded and located in or at the edge of diopside or anorthite.

The igneous crystallization sequence requires that AOIs experienced extensive melting; the small grain size indicates a high cooling rate, similar to that recorded by the thin overgrowth layers found on relict grains in CO3.0 chondrules. If the AOIs formed igneously and the diopside-anorthite intergrowths represent crystallized mesostasis liquid, then the round pores may represent contraction during crystallization; vapor-filled pores were surrounded by melt that solidified to a glass. Higher resolution images and consideration of surface-tension effects are required to interpret the porosity properly.



Our igneous scenario for AOI formation is essentially the same as the consensus model for chondrule formation. Interestingly, the low-FeO type-I chondrules in CO3.0 chondrites show similar porosity textures in their mesostases. This similarity in inferred formation models for AOIs and chondrules raises the question of why there is no recognizable glass in AOIs. We suggest that anorthite-diopside mixes are poor glass formers; this is consistent with the observations that calcic glasses devitrify more readily than sodic glasses. A related question is why the minerals, especially olivine, do not show euhedral faces. We suggest that the cooling rate was too high. The interlocking phase arrangement in AOIs (e.g., Fig. 1) is typical of those found in rapidly cooled liquids that crystallize several phases. We have observed rather similar structures in the small clouds of crystals (we suggested the name cauliflorets) sometimes found in the mesostasis regions of chondrules.

FABRIC ANALYSIS OF ALLENDE MATRIX USING EBSD.

L. E. Watt¹, P. A. Bland¹, S. S. Russell² and D. J. Prior³. ¹Dept. Earth Science & Engineering, Imperial College, London SW7 2AZ, UK. (lauren.watt@imperial.ac.uk). ²Dept. Min., Natural History Museum, London SW7 5BD, UK. ³Dept. Earth & Ocean Sciences, University of Liverpool, 4 Brownlow Street, Liverpool L69 3GP, UK.

Introduction: The abundant fine-grained matrix material in chondrites has limited the application of traditional fabric analysis techniques. Instead fabric analysis has been restricted to qualitative observations involving the large scale (>100 μ m) components of chondrites, e.g. flattened chondrules [1], and bulk meteorite studies using x-ray pole figure goniometry [2], magnetic susceptibility [3] and natural remnant magnetization [4]. Due to significant advances in microscopy, it has recently become possible to analyse the 3D crystallographic orientation of the fine-grained (sub-micron) matrix material in chondrites using an electron backscatter diffraction (EBSD) technique, thus allowing fabrics in these materials to be visualized for the first time [5].

EBSD Technique: EBSD is a scanning electron microscopy technique, in backscatter electron (BSE) mode, which permits the measurements of the full crystallographic orientation of any point [6]. BSE's that escape from the specimen will form a diffraction pattern that can be imaged on a phosphor screen. 3D crystallographic orientation data are obtained by automatically indexing these diffraction patterns, which are unique for any given phase. Samples are mapped by beam movement on a grid with a fixed step of 0.2 μ m to ensuring that each (sub) grain contains several measurement points. The EBSD technique enables the construction of orientation maps and the quantitative collation of data in a 3D sense using equal area, lower hemisphere pole figure plots of crystallographic orientations for a given area.

Results: Our work has focused on the analysis of the fine-grained, platy, fayalitic olivine in Allende matrix, of which multiple areas have been mapped using EBSD. Although the data are preliminary, several interesting features have been highlighted:

1. Fayalitic matrix olivines have a short a-axis. This differs to terrestrial and chondrule olivines which have a short b-axis.
2. There is a well developed 'short axis alignment fabric', which rotates around chondrule rims. Thus, platy olivine grains appear to 'tile' chondrules.
3. Any sample-scale fabric in the overall matrix, away from inclusions, is very weak.

Conclusions: The absence of a strong overall, sample-scale fabric in Allende, coupled with the presence of a well-developed chondrule rim fabric, would suggest that rim fabrics formed prior to their incorporation into the Allende host. The occurrence of a short a-axis in matrix olivines compared to a short b-axis in terrestrial [7] and chondrule olivines is likely to be explained by differences in their formation mechanisms. We are currently extending our EBSD analysis to investigate the alternative formation mechanisms for matrix olivine using experimentally generated samples. This will include looking at thermally and aqueously altered serpentinite samples and olivine condensates to see if we can recreate Allende fayalitic olivine crystallography.

References: [1] Tomeoka et al. 1999. *GCA* 63: 3683-3703; [2] Fujimura et al. 1983. *EPSL* 66: 25-32; [3] Sneyd et al. 1988. *Meteoritics* 23: 139-149; [4] Morden and Collinson. 1992. *EPSL* 109: 185-204; [5] Bland et al. 2003. *MAPS* 38: A100; [6] Prior et al. 1999. *Am. Min.* 84: 1741-1759; [7] Mizukami et al. 2004. *Nature* 427: 432-436.

UNRAVELING THE EXPOSURE HISTORIES OF AUBRITES. K. C. Welten¹, K. Nishiizumi¹, D. J. Hillebrand², M. W. Caffee^{2,3} and J. Masarik⁴, ¹Space Sciences Laboratory, University of California, Berkeley, CA 94720-7450, USA (e-mail: kwelten@uclink4.berkeley.edu); ²CAMS, Lawrence Livermore National Laboratory, Livermore, CA 94550, USA. ³Department of Physics, Purdue University, West Lafayette, IN 47907, USA, ⁴Nuclear Physics Department, Komensky University, Bratislava, Slovakia.

Introduction: Aubrites show very long cosmic-ray exposure (CRE) ages, up to ~120 Myr, which are poorly understood, since aubrites seem to be very fragile. Recent studies [1,2] revealed that many aubrites show large isotopic shifts in Sm and Gd due to neutron-capture reactions. These large isotopic shifts are believed to be mainly due to exposure on the aubrite parent body (APB) [2]. In this work we present ⁴¹Ca results in aubrites to determine the thermal neutron flux in space (4 π). We compare these fluxes with total neutron fluences [1,2] and noble gas CRE ages [3] to unravel the CRE history of aubrites in space (4 π) and on the APB (2 π).

Results and Discussion: Most aubrites show very low contributions of neutron-capture ⁴¹Ca (<0.1 dpm/gCa), indicating they were relatively small objects in space (R<30 cm). The only exceptions are Norton County (NC) and Cumberland Falls (CF), which show neutron-capture ⁴¹Ca contributions of 0.4-0.9 dpm/gCa (NC) and ~3 dpm/gCa (CF), respectively. The values in NC are much lower than those reported in [4], indicating our samples came from much closer to the surface (<5 cm). The high neutron-capture ⁴¹Ca in CF confirms that this aubrite had a large pre-atmospheric size [5]. Based on a CRE age of ~60 Myr for CF [3], we calculate a total thermal neutron fluence of ~1.5x10¹⁶ n/cm² during 4 - exposure. This value is still a factor of 2.7 lower than the one based on the Sm-Gd isotopic shifts [1]. Also for other aubrites, the total neutron fluences derived from neutron-capture ⁴¹Ca are lower than those given in [1,2]. This confirms that the high neutron fluences found in many aubrites can not be explained by exposure in space alone, but must be due to a previous exposure on the APB. Assuming that the aubrites were exposed at an average depth of ~150 g/cm² (at the maximum thermal neutron flux) on the APB, we find minimum 2 π -exposure ages of 24 Myr for NC, 45 Myr for Mayo Belwa (MB), 57 Myr for Bishopville, 70 Myr for Pesyanoe and ~105 Myr for CF. Despite significant exposure times on the APB, most of the ²¹Ne in NC and MB must have been produced during 4 -exposure, yielding 4 π exposure ages of 90-100 Myr.

An alternative explanation for the high Sm-Gd isotopic shifts in some aubrites is that they changed in size during their long irradiation in space, either due to a single break-up event or due to space erosion. We tested the space erosion hypothesis for our sample of NC, which came from <5 cm from the surface of an object with a pre-atmospheric radius of ~60 cm. We conclude that the neutron fluence of ~1.2x10¹⁶ n/cm² reported by [1] can be explained by a space erosion rate of ~0.5 mm/Myr, which is similar to the value of 0.65 mm/Myr for stone meteoroids determined in [6].

Conclusions. Many aubrites were exposed on the surface of the APB before irradiation in space. Despite a significant exposure on the APB, some aubrites still have long CRE ages as m-sized objects in space. This conclusion provides constraints on the collisional lifetime of aubrites and their delivery mechanism to Earth.

References: [1] Hidaka H. et al (1999) EPSL 173, 41-51. [2] Hidaka H. et al (2003) MAPS 38, A60. [3] Lorenzetti S. et al. (2003) GCA 67, 557-571. [4] Fink D. et al. (1992) LPSC 23, 355-356. [5] Welten K. et al. (2002) LPSC 33, #2043. [6] Schaeffer O. et al. (1981) Planet. Space Sci. 29:1109-1118.

NITROGEN-MAPPING AND NITROGEN-XANES SPECTROSCOPY OF INTERPLANETARY DUST PARTICLES.

S. Wirick,¹ G. J. Flynn,² L. P. Keller,³ and C. Jacobsen¹. ¹Dept. of Physics, SUNY-Stony Brook, Stony Brook, NY 11794, swirick@bnl.gov, ²Dept. of Physics, SUNY-Plattsburgh, Plattsburgh, NY 12901, ³NASA Johnson Space Center, Houston, TX 77058.

Introduction: We employ two Scanning Transmission X-Ray Microscopes (STXMs) on Beamline X1A of the National Synchrotron Light Source at Brookhaven National Laboratory to characterize the biologically important elements C, N, and O in interplanetary dust particles (IDPs). We map spatial distributions, at an ~50 nm scale, by comparing absorption maps taken above and below the element's K-edge, and we determine the functional groups by X-ray Absorption Near-Edge Structure (XANES) spectroscopy. The XANES results on 11 IDPs were reported by Flynn et al. [1]

Samples: Our first combined C, N, and O-XANES analyses, of two IDPs, one anhydrous and the other hydrated, and Murchison acid residue were described by Feser et al. [2]. We have now obtained N-, C-, and O-XANES spectra on ultramicrotome sections, each ~80 nm thick, of four IDPs, L2005*A3, L2006 #14 (a fragment from cluster 10), L2008U13, L2011R11, and we have obtained N- and C-XANES spectra on a fifth IDP, L2008H9.

Results: Three of the IDPs -- L2005*A3, L2011R11, and L2008U13 -- show similar N-XANES spectra, with broad pre-edge absorptions at ~400, ~402, and ~407 eV, indicating that the dominant N-carrier is the same in all three of these IDPs. In most cases the absorption at the N-edge is detectable but weak, indicating a relatively low N-concentration (near our detection limit of ~1% [2]). L2006 #14 has a strong absorption at the N-edge, but relatively weak pre-edge absorptions. In addition, the C-rich IDP, L2008H9, exhibits a strong N-edge absorption, and three strong pre-edge absorptions at ~400.9, 403.6, and ~406.7 eV (see Figure 1).

The images of L2008H9 taken above and below the N-edge were of sufficient quality to allow us to produce a N-map of this IDP. Surprisingly, the areas of high N-concentration do not correlate with the areas of highest C-concentration, suggesting that the organic carbon that we have detected in all IDPs examined to date [1] is not the dominant carrier of N, at least in L2008H9.

References: [1] Flynn, G. J. et al. 2003, *Geochim. Cosmochim. Acta*, **67**, 4791-4806. [2] Feser, M. et al. 2003, *34th Annual Lunar and Planetary Science Conference*, Abstract #1875.

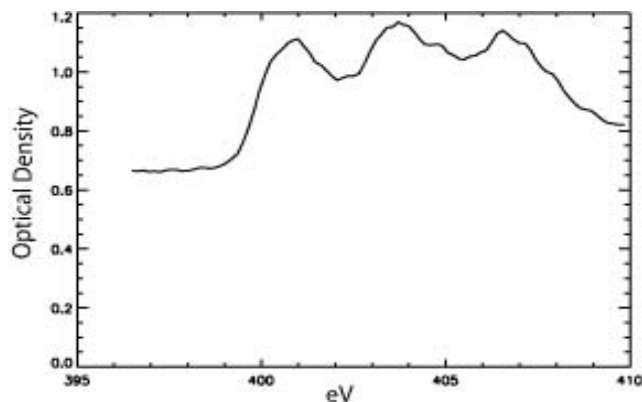


Figure 1: N-XANES spectrum of L2008H9, showing pre-edge absorption features.

FURTHER ANALYSIS OF THE Pd-Ag SYSTEMATICS OF SULPHIDES FROM THE GROUP IA IRON METEORITE CANYON DIABLO.

S. J. Woodland¹, M. Rehkämper¹ and A. N. Halliday¹, ¹Institut für Isotopengeologie & Mineralische Rohstoffe, ETH-Zentrum, Sonneggstrasse 5, Zürich, Switzerland. Woodland@erdw.ethz.ch, Markr@erdw.ethz.ch, Halliday@erdw.ethz.ch

Introduction: ¹⁰⁷Ag is produced by decay of the now extinct radionuclide ¹⁰⁷Pd ($t_{1/2} = 6.5$ Myrs). High Pd/Ag iron meteorites show good correlations between excess ¹⁰⁷Ag and Pd/Ag. This strongly indicates the presence of live ¹⁰⁷Pd at the start of the solar system [1]. Hence, the Pd-Ag chronometer is useful for studying early solar system processes such as planetesimal core formation. Isochrons determined for iron meteorites generally yield initial ¹⁰⁷Pd/¹⁰⁸Pd in the range $1.5 - 2.5 \times 10^{-5}$ [1]. Measurements of Canyon Diablo sulphide by [2] give the lowest ¹⁰⁷Ag/¹⁰⁹Ag yet measured for solar system material with $^{107}\text{Ag} = -12$ (where $\epsilon = [(\text{sample} / \text{standard}) - 1] \times 10000$) and have been used to estimate the initial solar system ¹⁰⁷Ag/¹⁰⁹Ag. This has been further investigated.

Methodology: Silver is separated from the sample matrix using low-blank (ca < 15pg/g) ion-exchange chromatography. Utilising MC-ICPMS, Ag isotopic compositions have been measured using both external normalization and sample-standard bracketing for mass bias correction. A reproducibility of 50 ppm (2 σ) can be obtained on ¹⁰⁷Ag/¹⁰⁹Ag for pure Ag standards [3].

Results: A single large sulphide (ca 17g) from Canyon Diablo (USNM 676) has been analysed several times. Despite a prior cleaning leach the initial results [4] yielded an isotopic composition identical, within uncertainty, to the terrestrial standard NIST SRM 978a. Two new measurements of the same sulphide have been undertaken using a more thorough cleaning procedure to ensure that any terrestrial contamination was removed. The samples were cleaned using a combination of abrasion by silicon carbide blocks and aqua-regia leaching. In total 17-19%, by weight, was removed from each sample during cleaning. The Ag isotopic compositions of the sulphide samples relative to the standard were $^{107}\text{Ag} = -0.4$ and $+0.4$ respectively. This agrees well with our original results and more extensive cleaning has no detectable effect on the Ag isotopic composition. Consequently, it is considered highly unlikely that any of these measurements are compromised by contamination. The composition of this Canyon Diablo sulphide is therefore concluded to be $^{107}\text{Ag} = -0.9 \pm 2.2$ (2 σ , n = 4). This is identical to the composition of the metal in which it is hosted. It is presently unclear why our Canyon Diablo sulphide has a Ag isotopic composition different to that measured by [2]. This disparity however, suggests that the Pd-Ag systematics of this meteorite are disturbed and that redistribution of Ag between sulphide and metal may have occurred. This has important implications regarding the use of Canyon Diablo sulphides to estimate initial solar system ¹⁰⁷Ag/¹⁰⁹Ag.

References: [1] Chen J. H. and Wasserburg G. J. (1996), in *Earth Processes: Reading the Isotopic Code*, Geophysics Monograph '95, p1-20. [2] Carlson R. W. and Hauri E. H. (2001), *Geochemica Cosmochimica. Acta*, 65: 1837-1848. [3] Woodland S.J. et al. (2003), in *Plasma Source Mass Spectrometry: Applications and Emerging Technologies*, Royal Society Of Chemistry, p338-350. [4] Woodland S. J. et al. (2003), Abstract #1621. 34th Lunar & Planetary Science Conference.

EVALUATION OF THE METEORITIC ALTERATION LEVEL USING THE SOLID-STATE CP/MAS ^{13}C NMR ANALYSES OF MACROMOLECULAR MATERIAL IN THE ANTARCTIC CARBONACEOUS CHONDRITES

H.Yabuta¹, H.Naraoka², K.Sakanishi³ and H.Kawashima³.
¹Arizona State University, Tempe, AZ 85287 USA. E-mail: H-karu.Yabuta@asu.edu ²Okayama University, Okayama, 700-8530, Japan. ³National Institute of Advanced Industrial Science and Technology, Tsukuba, 305-8569, Japan.

Introduction: Most of the organic matter in carbonaceous chondrites is present as insoluble macromolecular material which is known to be structurally and isotopically heterogeneous [1]. The chemical properties and structures of this insoluble material have been investigated by pyrolytic [2] or oxidative degradation [3] and solid-state ^{13}C -NMR [4,5], however, the history and the relationships between its constituents have not been revealed yet. In the present study, different carbon types were identified and quantified in the macromolecular material from Antarctic CM2 chondrites: [Yamato (Y) 74662, 791198, 793321; Belgica (B) 7904; Asuka (A) 881280, 881458]; and the Murchison meteorite by the solid-state CP/MAS ^{13}C NMR. The ratios of aromatic to aliphatic carbon (*Aro/Ali*) were estimated to evaluate the alteration level of each meteorite.

Experimental: Each powdered meteorite sample was demineralized repeatedly with 6N HCl and 8N HF/ 3N HCl, and then the carbonaceous material obtained was washed with methanol and dichloromethane. Elemental analyses were carried out by CHN elemental analyzer (Carlo Erba EA-1180).

Result and Discussion: The spectra of the macromolecular material of Murchison and Y791198 showed two broad peaks. One peak at 30 ppm was assigned to aliphatic carbon (*Ali-C*) that is a sum of CH_2 (at 33 ppm) and CH_3 groups (at 15 ppm). Another peak at 130 ppm was assigned to aromatic carbon (*Aro-C*). The spectra of the other meteorites showed only one major peak of *Aro-C*. Its width and a shoulder at the 60-80 ppm range probably corresponded the *Ali-C* linked to heteroatoms. Also, shoulders in the 150-180 ppm and 180-200 ppm ranges indicated the presence of carboxyl and carbonyl carbons, respectively.

The *Aro/Ali* was plotted to the H/C ratio from elemental analysis and a linear relationship was observed. The meteorites with lower H/C showed higher *Aro/Ali* and the ones with higher H/C showed lower *Aro/Ali*. Naraoka, et al. [6] proposed a new parameter for the thermal alteration event using H/C ratio of the macromolecular material. The correlation between *Aro/Ali* and H/C obtained in this study suggests that chemical structures of the macromolecular material in meteorites may reflect the thermal alteration level. It is proposed that aliphatic structures of the macromolecular material could have been aromatized or depleted during thermal alteration.

References: [1] Kerridge J. F. 1985. *Geochimica Cosmochimica Acta* 51:2527-2540. [2] Komiya, M. et al. 1993. *Geochimica Cosmochimica Acta* 57:907-914. [3] Hayatsu, R. et al. 1977. *Geochimica Cosmochimica Acta* 41:1325-1339. [4] Cronin, J. R. et al. 1987. *Geochimica Cosmochimica Acta* 51:299-303. [5] Cody, G. et al. 2002. *Geochimica Cosmochimica Acta* 66:1851-1865. [6] Naraoka H. et al. 2004. *Meteoritics & Planetary Science* 39: in press.

BASALTIC CLASTS IN LUNAR HIGHLAND BRECCIA YAMATO 86032.

A. Yamaguchi¹, H. Takeda², Y. Karouji³, and M. Ebihara^{1,3},
¹National Institute of Polar Research, Tokyo 173-8515, Japan (yamaguch@nipr.ac.jp), ²Research Institute, Chiba Institute of Technology, Narashino 257-0016, Japan, ³Department of Chemistry, Tokyo Metropolitan University, Hachioji, Tokyo 193-0397, Japan.

Introduction: Yamato (Y) 86032 is a feldspathic breccia from the lunar highlands, and is composed of at least three lithologies, white and light feldspathic lithology set in a dark-gray matrix (DG) and black impact melt veins [1]. We examined matrix components by optical and scanning electron microscopy and with an electron microprobe. The bulk composition of the DG was determined by ICP-MS and INAA.

Results and Discussion: The DG is composed of a wide variety of clasts such as glassy materials (devitrified impact melts and/or shock glass), granulitic breccias, basaltic components, and mineral fragments. The mineral fragments include plagioclase, pyroxene, olivine, silica minerals, Ti-rich or Al-rich chromite, and ilmenite [1]. Olivine compositions vary from Fo_{4.9-85.1}, the mg' of pyroxenes, 14.8-86.2, plagioclase compositions, An_{68.8-97.9}. These chemical variations imply a wider range of components from mare and highland than previously reported [2].

We found possible clasts of mare basalts. One of the mare basalt displays an ophitic texture, composed of plagioclase lath (<340 x 80 μm) and interstitial pyroxene with minor amount of silica, Ti-rich phases, and mesostasis. The other clast is brecciated and has a similar mineral assemblage. Pyroxene is widely zoned from core to rim (En_{4.7}Wo_{71.5} to En₁₀Wo₋₂₅₋₃₅), and shows a strong correlation between Fe/(Fe+Mg) and Ti/(Ti+Cr), distributing along as the similar range of VLT basalts [3]. These chemical variations in pyroxenes resemble to those of basaltic clasts in Y791197, but different from those in paired Y82192 [3,4]. There are many olivine and pyroxene fragments relatively rich in Fe. These Fe-rich clasts could be fragments of mare basalts although we cannot rule out the possibility that these clasts represent an extreme differentiate of highlands affinity.

Our bulk analyses generally indicate that the DG is mostly composed of the lunar highland components (Al = 16.0, Ca = 11.3, Fe = 4.09, and Ti = 0.14 wt%). The abundances of REEs are chondrite x2.5-4.4 with a positive Eu anomaly within the range of previous analyses [5]. Th (0.191 ppm) and U (0.0564 ppm) are extremely low, indicating the absence of KREEP components. This implies that this meteorite came from farside highlands, giving us an opportunity to study mare basalts of these regions.

References: [1] Yamaguchi A. et al. 2004. Abstract #1474 Lunar & Planetary Science Conference. [2] Takeda H. et al. 1990. *Proc. 20th Lunar Planet. Sci. Conf.*: 91-100. [3] Nielsen R.J. and Drake M.J. 1978, *Mare Crisium: The View from Lunar 24*. pp.419-428. [4] Goodrich C.A. et al. 1987. *Mem. NIPR, Spec. Issue 46*: 56-70. [5] Koeberl C. et al. 1989. *Proc. NIPR Symp. Antarct. Meteorites 2*:15-24.

**A TEST OF IMAGE PROCESS PROCEDURES OF
ASTEROID IMAGING CAMERA BY USING ITS
PROTOTYPE MODEL OF HAYABUSA (MUSES-C).**

A. Yamamoto¹, J. Saito², M. Ishiguro³, F. Yoshida⁴, S. Hasegawa⁵, H. Demura⁶, S. Kobayashi⁶, E. Nemoto⁶, Y. Murai⁶, K. Nishiyama⁶, M. Furuya⁶, and AMICA Science Team. ¹Remote Sensing Technology Center of Japan, E-mail: aya@restec.or.jp, ²Technical Research Institute, NISHIMATSU Construction Co. Ltd., ³Univ. of Hawaii, ⁴National Astronomical Observatory, ⁵JAXA, ⁶Univ. of Aizu

Introduction: Japanese Asteroid mission HAYABUSA (MUSES-C) was successfully launched at May 9th, 2003, and has been flying steadily towards a S-type asteroid "ITOKAWA". Although one of the main purpose of this mission is to bring back a sample from "ITOKAWA", but to get its surface information by using multiband camera (AMICA: Asteroid Multiband Imaging CAmera) and other instruments are also important [1][2]. We AMICA team has been examining its performance and data process procedures. For this purpose, we took the multiband images of several meteorites using AMICA Prototype Model (PM) in a laboratory.

Method and Instruments: AMICA PM has 7 filters which is similar to ECAS (Eight Color Asteroid Survey) systems. The center wavelength position of 7 filters are; 0.38 μm (ul-band), 0.42 μm (b-band), 0.54 μm (v-band), 0.7 μm (w-band), 0.86 μm (x-band), 0.94 μm (p-band) and 1 μm (z-band). We prepare the chips of 4 meteorites (Allende, Tuxtiac, Ingella Station and Gibeon). About 1-inch sized meteorites are molded in epoxy and sliced, then grounded by #600 and #1000.

Processed Images: Original data are normalized to DN/msec, and divided by STD (SpectralonTM) for cancellation of CCD response and light source energy curve. From these processed data, we made a simulated true color composite image (RGB: w-band, v-band, b-band) and color ratio map [3] to examine the performance of AMICA PM. Color difference of each meteorite sample are confirmed by true color composite image. Chondrules and matrix in the Allende can be distinguished in color ratio map of b-band / w-band. This result will support us for construction of image processing procedures for ITOKAWA observation.

References: [1] Kawaguchi J. and Uesugi K. 1999. IAF-99-IAA.11.2.02, 50th International Astronautical Congress, 1-9. [2] Nakamura T. et al. 2001. Earth Planets Space 53:1047-1063. [3] Pieters C. M. et al. 1994. Science 266:1844-1848.

SIGNIFICANT DEPLETION OF ARGON-RICH NOBLE GASES IN THE NINGQIANG CARBONACEOUS CHONDRITE DURING EXPERIMENTAL AQUEOUS ALTERATION

Y. Yamamoto, R. Okazaki, and T. Nakamura. Department of Earth and Planetary Sciences, Kyushu University, Fukuoka 812-8581, Japan. E-mail: yamamoto@geo.kyushu-u.ac.jp

Introduction: Ar-rich noble gases are a main component of primordial noble gases in unequilibrated ordinary chondrites and some classes of anhydrous carbonaceous chondrites [e.g., 1]. The Ar-rich gases are characterized by the high $^{36}\text{Ar}/^{132}\text{Xe}$ and $^{84}\text{Kr}/^{132}\text{Xe}$ ratios relative to Q gas [2]. Recently it is reported that the Ar-rich gases are removed by light HF/HCl etching, like solar wind noble gases, and thus suggested that they locate in the amorphous rims around fine-grained olivine and pyroxene [3]. On the other hand, the Ar-rich gases are minor in carbonaceous chondrites that experienced aqueous alteration [e.g., 4]. In order to understand the relation between the abundance of Ar-rich gas contents and the degree of aqueous alteration that meteorite experienced in their parent bodies, we performed an experimental aqueous alteration on Ningqiang. A piece weighing 0.3g was crushed into μm -sized particles and kept in liquid water at 200°C for 10 and 20 days. Natural Ningqiang sample and altered ones soaked for 10 and 20 days were analyzed for mineralogy by X-ray diffraction and for noble gases by stepped pyrolysis.

Results and Discussion: Mineralogical analysis shows that the natural sample consists of olivine, low-Ca pyroxene, magnetite and troilite. Olivine, low-Ca pyroxene and troilite contents were reduced in the sample altered for 10 days, while phyllosilicate and hematite formed. Noble gas analyses show that the experimental alteration for 10 days removed 90, 72 and 61% of ^{36}Ar , ^{84}Kr and ^{132}Xe , respectively, whereas lesser proportion (28%) of ^{20}Ne was removed. The $^{36}\text{Ar}/^{132}\text{Xe}$ and $^{84}\text{Kr}/^{132}\text{Xe}$ ratios were reduced from 220 and 1.3 to 59 and 0.9, respectively, whereas $^{20}\text{Ne}/^{132}\text{Xe}$ ratio was increased from 31 to 57. Calculated $^{36}\text{Ar}/^{132}\text{Xe}$ and $^{84}\text{Kr}/^{132}\text{Xe}$ ratios of noble gases removed by the alteration are 323 and 1.5, respectively, and are in the range of Ar-rich gases in enstatite chondrites [5] and ureilites [6]. These indicate that the Ar-rich gases are located in materials that are very susceptible to weak aqueous alteration brought about by the neutral water. In contrast, the noble gases remaining in the sample are close to Q gas in the elemental compositions. This indicates that Q gas in phase Q is much more resistant to aqueous alteration than the Ar-rich gases. In the sample altered for 20 days, mineralogy and noble gas signatures are basically similar to the 10-day sample, indicating that most of the Ar-rich gases were lost by aqueous alteration within 10 days. Our results suggest that major portion of primordial noble gases were lost from primitive hydrous asteroids during low-temperature aqueous alteration.

References: [1] Schelhaas N. et al. 1990. *Geochimica et Cosmochimica Acta* 54:2869-2882. [2] Wacker J. F. and Marti K. 1983. *Earth and Planetary Science Letters* 62:147-158. [3] Nakamura T. et al. 2003. *Meteoritics & Planetary Science* 38:243-250. [4] Nakamura T. et al. 1999. *Geochimica et Cosmochimica Acta* 63:241-255. [5] Crabb J. and Anders E. 1981. *Geochimica et Cosmochimica Acta* 45:2443-2464. [6] Wacker J. F. 1986. *Geochimica et Cosmochimica Acta* 50:633-642.

METALLOGRAPHIC COOLING RATE METHODS: APPLICABILITY TO SPECIFIC TEMPERATURE RANGES DURING COOLING.

J. Yang¹ and J. I. Goldstein¹, ¹Dept. of Mechanical and Industrial Engineering, University of Massachusetts, Amherst, MA 01003, USA, jiyang@ecs.umass.edu and jig0@ecs.umass.edu.

Introduction: Cooling rates obtained by a variety of metallographic methods can reveal the thermal history of the asteroids and in some cases the size of the meteorite parent bodies. However, cooling rates obtained by different cooling rate methods are valid only for a specific temperature range [1, 2]. The importance of this phenomenon is discussed.

Metallographic Cooling Rate Methods: In general, the metallographic cooling rate methods are either kamacite-based [3-5] or taenite-based [6-11]. The kamacite-based methods are very sensitive to the temperature-composition value of the α/γ +(Ph.) phase boundary in the Fe-Ni and Fe-Ni-P systems and the results are often inaccurate. On the other hand, taenite-based methods are reliable. In addition, taenite-based methods allow one to obtain cooling rates in specific cooling temperature ranges.

Cooling Temperature Ranges: The determination of the applicable cooling temperature ranges depends on several factors: cooling rate method, cooling rate, and meteorite composition. The meteorite composition controls the effect of the Fe-Ni and Fe-Ni (P saturated) phase diagrams, inter-diffusion coefficients and kamacite nucleation mechanism. For example, the taenite central Ni method [6, 7] or taenite profile matching method [8] gives cooling temperature ranges from ~600 to ~380 C in chemical group IIIA, from ~700 to ~380 C in chemical group IIIB, and from ~580 to ~380 C in chemical group IVA. The cooling temperature range in H chondrites varies from ~700 to ~380 C based on the taenite central Ni method, although grain boundary nucleation and diffusion may be more important [12]. The tetrataenite rim method [10] measures the cooling rate in the temperature range from 380 to 350 C in iron and stony iron meteorites and from 400 to 350 C in stony meteorites. The cloudy zone method [11] measures the cooling rate in the temperature range from 320 C to below 0 C and can be applied in iron, stony iron and stony meteorites. The realization that there is a significant difference in the applicable temperature ranges in chemical group IIIAB raises a concern about the nature of the IIIAB parent body based on past cooling rate calculations [3, 13]. If the measured cooling rates are not all obtained from the same temperature, a uniform cooling rate does not necessarily imply a core for the parent body. On the other hand, non-uniform cooling rate does not necessarily mean that the meteorites are distributed within the parent body. Direct experiments and calculations based on either the tetrataenite rim method or the cloudy zone method can give us new evidence about the structure of the parent body. These two methods give cooling rates at a uniform cooling temperature range for iron, stony iron and stony meteorites and are independent on the composition of the bulk metal.

References: [1] Haack H. et al. 1994. *Meteoritics* 29:470-71. [2] Yang J. et al. 2004. Abstract #1288. 35th Lunar & Planetary Science Conference. [3] Goldstein J.I. et al. 1967. *GCA* 31:1733-70. [4] Willis J. et al. 1978. *EPSL* 40:162-67. [5] Haack H. et al. 1996. *GCA* 60:2609-19. [6] Wood J.A. 1964. *Icarus* 3:429-59. [7] Rasmussen K.L. 1981. *Icarus* 45:564-76. [8] Goldstein J.I. et al. 1965. *GCA* 29:893-920. [9] Short J.M. et al. 1967. *Science* 156:69-61. [10] Yang et al. 2003. unpublished. [11] Yang C-W et al. 1997. *GCA* 61:2943-56. [12] Reisener R.J. et al. 2003. *MAPS* 38:1679-96. [13] Rasmussen K.L. 1989. *Icarus* 80:315-25.

IMPACT GLASSES AS CHRONOSTRATIGRAPHIC BENCHMARKS OF THE LATE CENOZOIC PAMPEAN RECORD, ARGENTINA

M. A. Zárate¹, P. H. Schultz², W. Hames³, C. Heil⁴ and J. King⁴

¹CONICET-UNLPAM, Avenida Uruguay 151, 6300 Santa Rosa, La Pampa, Argentina E-mail: mzarate@exactas.unlpam.edu.ar

²Department of Geological Sciences, Brown University, Providence, RI 02912-1846 USA, ³Auburn University, Auburn, AL 36830 USA, ⁴University of Rhode Island, Narragansett, RI 02882, USA.

The Late Cenozoic continental record of the Pampas is dominantly composed of massive sandy siltstones, usually reported as loess and loess-like (loessoid) deposits [1]. The abundant vertebrate fossil remains found in the sediments have been grouped into the Chasicuan, Huayquerian, Montehermosan, Chapadmalalan, Marplatan, Ensenadan, and Lujanian South American Land Mammal ages (SALMAS) on the basis of their relative degree of evolution [2] [3]. Until recently, the sequence was poorly time-constrained. However, the identification and characterization of meteorite impact glasses ('escorias') [4] [5] have recently provided a chronostratigraphic tool to chronologically calibrate the succession.

Within these deposits, five impact-glass horizons, extending from the Pleistocene to the late Miocene have been reported [5]. Glasses are usually highly vesicular occurring at relatively discrete layers. Secondary reworked impact glass facies are found stratigraphically above the primary layers. Evidence for an impact origin includes mineral constituents and textures, while the geochemical signature of each event suggests a variable depth of impact excavation [5].

Radiometric ages were obtained by high resolution ⁴⁰Ar/³⁹Ar dating [4] [5]. The oldest impact glass horizon occurs within Chasicuan sediments yielding an age of 9.23±0.09 Ma. A more recent late Miocene impact glass layer of 5.33± 0.05 Ma was found in Huayquerian deposits near Bahía Blanca. A 3.27± 0.08 Ma impact glass horizon, traceable along several kilometers, occurs at the uppermost section of the Chapadmalalan beds near Mar del Plata. Two other Pleistocene impact glass layers were found at Centinela del Mar, about 60 km southwest of Mar del Plata in a succession bearing Marplatan and Lujanian fossil vertebrates. The upper glass horizon yielded an age of 445 ± 21 ka and the lower glasses 230±30 ka. The stratigraphic inconsistency of the ages is likely related to some local redeposition. When compared to previous chronological interpretations [3] [6], the impact glass layers provided independent ages that served to re-adjust the chronology attributed to the SALMAS, thereby suggesting different time interval for the fossil vertebrate associations.

References:[1] Zárate, 2003 *Quaternary Science Reviews* 22:1987-2006. [2], R. Pascual et al. 1965. *Anales Comisión de Investigaciones Científicas de la Provincia de Buenos Aires*, 6: 165-193. (3) A. Cione et al. 2000. *INSUGEO, Serie Correlación Geológica* 14: 191-237, [4] Schultz et al., 1998, *Science* 282:2061-2063 [5] Schultz, P.H et al. 2004. *Earth and Planetary Science Letters* 219:221-238. [6] J. Flynn, and C.C Swisher III, 1995. *Society for Economic Paleontologists and Mineralogists Special Publication* 54: 317-333.

APXS ANALYSES OF BOUNCE ROCK – THE FIRST SHERGOTTITE ON MARS.

J. Zipfel¹, R. Anderson², J. Brückner¹, B. C. Clark³, G. Dreibus¹, T. Economou⁴, R. Gellert^{1,5}, G. Klingelhöfer⁵, G. W. Lugmair¹, D. Ming⁶, R. Rieder¹, S. W. Squyres⁷, C. d'Uston⁸, H. Wänke¹, A. Yen², and the Athena Science Team.

¹MPI für Chemie, Mainz, Germany. e-mail: zipfel@mpch-mainz.mpg.de.

²JPL, Pasadena, CA, USA. ³Lockheed Martin, Littleton, CO, USA.

⁴LASR, Enrico Fermi Institute, Chicago, IL, USA. ⁵J. Gutenberg-Universität Mainz, Germany.

⁶JSC, Houston, Tx, USA. ⁷Cornell University, Ithaca, NY, USA. ⁸CESR, Toulouse, France.

Introduction: During the MER Mission, an isolated rock at Meridiani Planum was analyzed by the Athena instrument suite [1]. Remote sensing instruments noticed its distinct appearance. Two areas on the untreated rock surface and one area that was abraded with the Rock Abrasion Tool were analyzed by Microscopic Imager, Mößbauer Mimos II [2], and Alpha Particle X-ray Spectrometer (APXS). Results of all analyses revealed a close relationship of this rock with known basaltic shergottites.

APXS results: The APXS analysis on the abraded area (Glanz2) of Bounce Rock is shown in the Table. In addition, an analysis of a typical basalt (Humphrey) as found in Gusev crater is shown. While Gusev basalts have a very primitive nature with low SiO₂ and high MgO contents, Bounce Rock has the composition of more evolved basalts. It also has a chemical signature typical of basaltic shergottites: a high P₂O₅ content, a S content of 0.2 wt.%, a Fe/Mn ratio of 36.2 in close agreement with other shergottites (Fe/Mn = 36-44), a low mg-value of 0.42, and a high Ca/Al ratio of 1.7. Element concentrations fall well within the range of typical basaltic shergottites, with the exception of lower FeO and higher CaO and Br. Al₂O₃ concentrations and mg-values - both known to span a wide range in shergottites - are identical in Bounce Rock and lithology B of EETA79001 (EET-B). The resulting mineralogy is strongly pyroxene-normative: (in wt.%) magnetite 0.25, ilmenite 1.4, chromite 0.2, apatite 2.0, albite 12.7, anorthite 22.0, diopside 31.1, hypersthene 30.5.

	Humphrey RAT2	Bounce Rock Glanz2	EETA 79001 Lith. B	Sher- gotty	Zagami	QUE 94201
ref.	[3]		[4]	[4]	[4]	[5]
SiO ₂	45.7	50.8	49.0	51.4	50.8	48.0
TiO ₂	0.53	0.78	1.1	0.87	0.77	1.8
P ₂ O ₅	0.59	0.95	1.3	0.80		
Al ₂ O ₃	10.6	10.1	9.93	7.06	5.67	12.0
Cr ₂ O ₃	0.59	0.12	0.18	0.20	0.30	0.13
MnO	0.38	0.43	0.45	0.53	0.50	0.44
FeO	18.0	15.6	17.7	19.4	18.0	18.3
MgO	11.5	6.5	7.4	9.3	11.0	6.2
CaO	7.53	12.5	11.0	10.0	10.8	11.3
Na ₂ O	2.8	1.25	1.66	1.29	0.99	1.75
K ₂ O	0.08	0.10	0.065	0.16	0.14	0.05
Ni ppm	190	<120	46	83	67	<20
Zn ppm	120	50	120	83	62	130
Br ppm	50	30	0.287	0.890	0.870	0.350
Sum	99.50	99.55	99.86	100.96	98.97	99.97

Conclusion: Bounce Rock chemically closely resembles basaltic shergottites, in particular to EET-B. This, and results from the other instruments, provide further evidence that "Martian" meteorites do indeed come from Mars.

Reference: [1] Squyres S. W. et al. (2003), *J. Geophys. Res.*, **108** (E12), 8062, doi:10.1029/2003JE002121. [2] Rodionov D. et al. (2004), this issue. [3] Gellert et al. (2004) *Science*, subm. [4] Banin et al. (1992) In *Mars*, 594-625. [5] Dreibus et al. (1996) *MAPS* **31** (Suppl.), A39-A40.

FLUID INCLUSIONS IN CHONDRITES

M. Zolensky¹, R. Bodnar², A. Tsuchiyama³, K. Okudaira⁴, T. Noguchi⁴, K. Uesugi⁵ and T. Nakano⁶. ¹NASA Johnson Space Center, Houston, TX 77058 USA (michael.e.zolensky@nasa.gov). ²Department of Geosciences, Virginia Polytechnic University, Blacksburg, VA 24061 USA. ³Department of Earth and Space Science, Osaka University, Toyonaka, 560-0043 Japan. ⁴Department of Materials and Biological Science, Ibaraki University, Ibaraki 316-8511, Japan. ⁵JASRI/Spring 8, Hyogo, Japan. ⁶Geological Survey of Japan, Tsukuba, 305-8567 Japan.

Introduction: We report progress in our search for aqueous fluid inclusions from within chondrites, building on our discovery of them within halite and sylvite crystals in the Monahans (1998) and Zag H5 regolith breccias [2].

How to search for fluid inclusions: Given that many extraterrestrial materials have experienced extensive aqueous alteration, why have aqueous fluid inclusions not been reliably reported there before? Here is why: (1) Practically all samples are prepared using water, with obvious results. (2) Most thin sections are heated during preparation, resulting in the decrepitation (destruction) of most fluid inclusions. (3) Practically all prepared samples are studied using electron- or ion-beam instruments, resulting in further heating and inclusion homogenization and/or decrepitation. (4) Most fluid inclusions are very small, and single phase (fluid only), rendering them almost indistinguishable from other growth defects.

Here are the procedures we have learned to take: (1) Use the freshest, least terrestrially-altered specimens available. (2) Prepare all thin sections using alcohol as the only fluid, and grind and polish very slowly to inhibit heating. (3) Examine separated grains rather than thin sections whenever possible. (4) Freeze all samples before examination, to promote nucleation of vapor bubbles in otherwise single-phase inclusions, so that fluid inclusions can be more easily identified.

Potential fluid inclusions: In the past we have been locating potential fluid inclusions in CM chondrite olivine and carbonates. We have lately been concentrating on carbonates in the CI chondrites Orgueil and Ivuna, using standard petrographic and computerized X-ray microtomographic techniques (X-ray CT). Orgueil carbonates contain few if any fluid inclusions, all of which are very tiny (~1-5 microns at most), while Ivuna Ca-Mg carbonates frequently contain them. The potential fluid inclusions in Ivuna are commonly under 2 micrometers in diameter, but range up to many 10's of microns in places. It is possible that Orgueil has experienced too severe brecciation [2] to have preserved fluid inclusions in such unresilient minerals as carbonates. To test this we are doing X-ray CT imaging of Orgueil sulfide crystals. We are now examining all potential fluid inclusions by Raman microspectrometry.

References: [1] Zolensky et al. (1999) *Science* **285**, 1377.
[2] Endreß and Bischoff (1993) *Meteoritics* **28**, 345.

PATHWAYS OF HYDROGEN GENERATION DURING AQUEOUS ALTERATION OF CHONDRITES

M. Yu. Zolotov¹ and E. L. Shock^{1,2}. ¹Department of Geological Sciences, ²Department of Chemistry/Biochemistry, Arizona State University, Tempe, AZ 85287. E-mail: zolotov@asu.edu.

Formation, phase separation, and escape of gases during aqueous alteration of asteroids affected pressure and redox conditions in their interiors [1-5]. Although formation of H₂ in asteroids has been predicted [1-4], conditions and pathways of H₂ generation have not been thoroughly explored. We review the potential for H₂ production through aqueous oxidation of Fe-Ni metal, ferrous silicates, and troilite. In the framework of these pathways, production of H₂ depends on temperature, pressure, the amount, ionic strength, pH, and oxidation state of solution; the amount, composition, and grain size of minerals, as well as on the ability of H₂ to leave the reaction zone.

The Fe⁰-H₂O(l) equilibrium cannot be attained and water-Fe⁰ interactions in asteroids proceeded until either the metal (as in CI carbonaceous chondrites), or the H₂O (as in ordinary chondrites) was exhausted. Alkaline fluids [1,4] favored formation of magnetite via reaction $3\text{Fe}^0 + 4\text{H}_2\text{O}(\text{l}) \rightarrow \text{Fe}_3\text{O}_4 + 4\text{H}_2$ (1) and an age of magnetite in the Orgueil CI chondrite [6] is consistent with rapid H₂ generation. In neutral and alkaline solutions, the pH does not affect the rate of reaction (1), but several other factors (absorption of H₂, presence of organic species, low water activity, and inability of H₂ to escape) could make the process slower. Although reaction (1) can be regarded as a major source of H₂, formation of Ni-rich metal alloys at advanced stages of the alteration would retard the process of metal oxidation.

Formation of fayalitic olivine at the expense of Fe⁰ and SiO₂(aq) and formation of tochilinite through alteration of FeS and Fe⁰ provide two more plausible sources of H₂. However these reactions produce only 1 mole of H₂ per 1 mole of Fe⁰ reacted, less than reaction (1) does. Aqueous conversion of enstatite to ferrous olivine [7] is a less important source of H₂.

Once Fe⁰ is consumed, the amount of H₂ could be stabilized by achieving equilibrium among magnetite and fayalite: $\text{Fe}_3\text{O}_4 + \text{SiO}_2(\text{aq}) + \text{H}_2 \leftrightarrow 1.5\text{Fe}_2\text{SiO}_4 + \text{H}_2\text{O}(\text{l})$ (2). For example, formation of H₂ in hot zones could be compensated by H₂ consumption through the Fe₃O₄→Fe₂SiO₄ conversion in colder zones, consistent with observations [e.g., 3]. Equilibrium (2) can be achieved only at relatively low values of *f*H₂, which may imply escape of H₂ produced by reactions with Fe⁰. Fayalite-magnetite assemblages observed in ordinary chondrites and in CV3 carbonaceous chondrites [e.g., 3] indicate the possibility of such equilibration, at least at the ηm-mm scale. Note that Fe₃O₄-FeS equilibration could also participate in the buffering of H₂.

Oxidation of Fe^(II)-silicates (e.g., the reverse of reaction 2) may not be the *primary* source of H₂, because Fe-rich silicates form in many cases through aqueous alteration on parent bodies, consistent with mineral substitution patterns, oxygen isotope data, and isotopic dating.

References: [1] Browning L. and Bourcier W. 1996. *Meteoritics & Planetary Science* 31:A22-A23. [2] Petaev M. I. and Mironenko M. V. 1997. In LPI Tech. Rept. No. 97-02, 49-50. [3] Krot A. N. et al. 1998. *Meteoritics & Planetary Science* 33:1065-1085. [4] Rosenberg N. D. et al. 2001. *Meteoritics & Planetary Science* 36:239-244. [5] Wilson L. et al. 1999. *Meteoritics & Planetary Science* 34:541-557. [6] Pravdivtseva O. V. et al. 2003. Abstract #1863. 34th Lunar & Planetary Science Conference. [7] Krot A. N. et al. 2003. *Meteoritics & Planetary Science* 38:A73.

BRAZILIAN METEORITES

M. E. Zucolotto¹, L.L. Antonello¹. Museu Nacional, Rio de Janeiro, Brazil, zucoloto@acd.ufjf.br

The research project "Brazilian Meteorites" carrying out in Museu Nacional/UFRJ, Rio de Janeiro, involve: geologists, astronomers and students, as well as amateur astronomers interested in such a matter in Brazil. Even without any financial support, it had some progress in view of twelve new meteorites became to the knowledge of Science and two new other masses to be analyzed. Some errors concerning the meteorite's classification, pointed out by Buchwald [1], has been solved and others not yet.

None of Brazilian meteorites has their strewnfield determined, not even those that fell more recently as Campos Sales (1991). Otherwise, most of Brazilian meteorites have only a mass recovered. As it well known that single falls are a very rare event, many places of falls were visited trying to find more samples, but the only award brought is the correct historical data. These histories will be published soon in a book concerning to Brazilian Meteorites by the present authors.

On visits to the localities former divulgated [2] is very common heard about of previous foreign dealers activities. For instance, with one Paranaíba mass, a dealer mislead the elderly meteorite owner substituting the authentic meteorite for a "hot rock". Even in Universities and small collections some meteorites have completely disappeared (e.g. 20 kg of Conquista from UFMG and quite the whole Djalma Guimarães Collection). Some Universities had the meteorites in private possession of the retired curator for protection. This lead to many retired curators to put the University's collection under their own responsibility.

In spite of many talks have been performed focusing to amateurs astronomers groups and Universities, the lack of the knowledge by the great population induces to its barely contribution with few new meteorites recovering. This is the result where a country with such continental dimension as Brazil has, solely were registered 54 meteorites. Minas Gerais State (MG) has about a third of them, possibly due to the most interest of the native population in ore discovery.

Even so, Brazil is awarded with very rare and singular meteorites, as **Angra dos Reis, RJ**. (Angrite), **Ibitira, MG**. (Vesicular Eucrite), **Governador Valadares, MG**. (Nakhlite), **Santa Catarina** (Ni richest ataxite), **São João Nepomuceno** (IVA stony-iron) and **Bocaiuva, MG** (silicate rich iron) which performs more than 10% of the Brazilian meteorites.

MG	Barbacena, Bocaiuva, Conquista, Governador Valadares, Ibitira, Indianópolis, Itutinga, Maria da Fé, Minas Gerais, Pará de Minas, Paracutu, Patos de Minas I, Patos de Minas II, Patrimônio, Piedade do Bagre, Pirapora, S. João Nepomuceno, Sete Lagoas, Uberaba.		
GO	Itapuranga, Sanclerlândia, Santa Luzia, Uruaçu, Veríssimo.		
RS	Nova Petrópolis, Putinga, Santa Bárbara, Soledade.		
SC	Blumenau, Mafra, Morro do Roccio, Santa Catarina.		
RJ	Angra dos Reis, Angra dos Reis II, Casimiro de Abreu.		
SP	Avanhandava, Marília, S. José do Rio Preto.		
BA	Bendegó, Quijingue, Rio do Pires.		
CE	Campos Sales, Cratheus, Parambú.		
PR	Iguaçu, Ipiranga, Rio Negro.	RN	Macau
MA	Balsas, Itapicuru-Mirim.	PE	Serra de Magé
MT	Cacilândia, Paranaíba.	PA	Ipitinga

References:

[1] Buchwald, F.V. (1975). Handbook of Iron Meteorites. [2] Gomes, C.B. & Keil, K. (1980). Brazilian Stone Meteorites. Univ. of New Mexico Press.

THE SÃO JOÃO NEPOMUCENO, IVA STONY-IRON.

M. E. Zucolotto¹ and L. L. Antonello¹. Museu Nacional/UFRJ-
Rio de Janeiro - Brazil - zucoloto@acd.ufrj.br.

A mass of about 15 kg was found at vicinities of São João Nepomuceno (Minas Gerais State) and donated in 1960 to Museu Nacional, Rio de Janeiro. In 1973 one half of the meteorite was donated to Smithsonian Institution. The main mass was elongated with the average dimensions 19.5x10x9.5 cm and significantly weathered.

In polished and etched sections it displays a messy texture of metal and silicates, with the latter comprising about 20% of the surface area heterogeneously distributed, preferentially on parent taenite crystals grain boundaries. Those silicate-rich regions resemble those in the stony-iron Steinbach.

The metal matrix shows a beautiful polycrystalline fine Widmanstätten structure, with long kamacite bands of 0.30-0.05 mm wide. Kamacite shows Neumann bands and micro hardness HV 170-15. Taenite and plessite cover around 50% of the area. Many kinds of plessite fields typical of IVA irons are present.

Terrestrial corrosion has selectively attacked along Widmanstätten grain boundaries and fissures. It presents many aggregates of austenite grains, ranging from few mm to 8 cm in diameter. Many individual grains are separated by a 0.6-0.9 mm wide grain boundary of kamacite ribbons and others grains by the silicate-bearing rich areas. Troilite have been shock-melted but taenite and plessite exhibited undisturbed M-profiles. Neither Schreibersite nor rhodite were observed.

Polished thin sections present a silicate texture assemblage constituting by ortho and clino bronzite and tridymite; they occur in mutual contact altogether with troilite.

SJN is unusual in their content of silicates and is close related to Steinbach. The SB is richer in silicates (50%), and was classified as stony-iron [1] and from high Ni-IVA trend. The SJN contains less silicate (~20%), from low-Ni IVA trend and is also classified by many authors as stony-iron.

Group IVA is the most extensively debated iron meteorite group in terms of metallographic cooling rates [2-7]; indeed it remains enigmatic with a thermal evolution quite different from other magmatic irons.

SJN is one of silicate-rich bearing IVA irons that exhibits minerals with density differences not supported in asteroidal core models with very slow cooling rates. The breakup and reassembly model [7] try to explain the complexity of the IVA irons, in special SJN and ST as could provide hot and cold fragments thermally equilibrated and ejected debris reaccumulated.

A new focus on the matters should be considered, that is the solidification of iron and stony-iron meteorites from a melt under microgravity conditions [8]. Here the melted target material may have formed two immiscible liquids (metal-sulfide and silicate) in a related process involving little density separation. In this case the polycrystalline assemblage of the São João looks like a welded breccia, possibly formed by a catastrophic fragmentation and reassembled under microgravity condition.

References: [1] Döfler *et al.* (1965). *Min.Pet.Mitt.* 16:413-429. [2] Reid *et al.* (1974). *EPSL*, 22:67-74. [3] Bild, R.W. & Wasson, J.T. (1976). *Min.Mag.* 40: 721-735. [4] Prinz *et al.* (1984) *MAPS*. 19:291-292. [5] Schaudy *et al.* (1972). *Icarus*. 17:174-192. [6] Rasmussen *et al.* (1995). *GCA* 59:3049-3059. [7] Scott *et al.* (1994), *Meteoritics*. 29: 530-531. [8] Budka *et al.* (1996). *The Minerals, Metals & Material Society*, 49-57.